

Zhen Wang, Qifeng Shu\* and Kuochih Chou

# Study on Structure Characteristics of $B_2O_3$ and $TiO_2$ -bearing F-Free Mold Flux by Raman Spectroscopy

**Abstract:** Structure characteristics of fluoride-free mold flux containing simultaneously  $B_2O_3$  and  $TiO_2$  have been investigated by Raman spectroscopy in this work. Raman spectra for glass samples with different basicities, different contents of  $TiO_2$  and  $B_2O_3$  were recorded during the experiments. According to the experiments results, increase of  $TiO_2$  content leads to the appearance of  $[TiO_4]$  and  $[TiO_6]$  structure groups, and  $[TiO_4]$  becomes the main structure unit in the system.  $TiO_2$  produces a certain destructive effect on Si-O-Si network structure as well as large borate group and conducive to the formation of some other complex structure groups, such as (Si,Ti) coupling in sheet unit. It can be concluded that, with the increase of  $B_2O_3$ , the ratio of mixing of the  $Q^0$  structure unit and  $[TiO_4]$  structural group decrease and the ratio of sheet structure unit increase, and there forms large borate group. Existence of  $B_2O_3$  increases polymerization degree of the slag system. In addition, increasing basicity causes to the decrease of  $Q^2$  and sheet structure unit and increase of mixing of the  $Q^0$  structure unit and  $[TiO_4]$  structural group, and weakening the large borate group. It could be concluded that the increase of basicity reduces the degree of polymerization of the system.

**Keywords:** fluoride-free mold flux,  $B_2O_3$  and  $TiO_2$ , structure, raman spectroscopy

**PACS® (2010).** 61.20.Qg

**Zhen Wang:** State Key Laboratory of Advanced Metallurgy, University of Science and Technology Beijing, Beijing 100083, China; School of Metallurgical and Ecological Engineering, University of Science and Technology Beijing, Beijing 100083, China

**\*Corresponding author: Qifeng Shu:** State Key Laboratory of Advanced Metallurgy, University of Science and Technology Beijing, Beijing 100083, China; School of Metallurgical and Ecological Engineering, University of Science and Technology Beijing, Beijing 100083, China  
E-mail: shuqifeng@gmail.com

**Kuochih Chou:** State Key Laboratory of Advanced Metallurgy, University of Science and Technology Beijing, Beijing 100083, China; School of Metallurgical and Ecological Engineering, University of Science and Technology Beijing, Beijing 100083, China

## 1 Introduction

As critical materials in continuous casting process, mold flux plays an irreplaceable role in metallurgical industry. However, the fluorides within traditional mold flux produce harmful influence both on the natural environment and on equipment seriously, such as, volatilization of fluorides leading to erosion to continuous caster, pollution of environment, acidification of the cooling water, human health hazard, and so on [1–4]. Thus, the development and application of fluorine free mould flux is of great significance and has become a research area of interest [2–5]. It is reported that slags bearing  $B_2O_3$  and/or  $TiO_2$  become most promising substitute for traditional mould fluxes [2–8]. According to some previous studies [2, 4, 7, 8], the existence of  $TiO_2$  in mould fluxes can easily lead to the formation of some crystals (eg.  $CaTiO_3$  or  $CaO \cdot SiO_2 \cdot TiO_2$ ) with high melting point, which is potential to replace the cuspidine generated by fluorine in mould fluxes to ensure the crystallizability of slag to achieve good heat transfer performance. Besides,  $B_2O_3$ , as an effective fluxing agent to lower the melting point of mould flux, has been taken into consideration for being added to mould fluxes to adjust the viscosity or melting properties of slag [3, 5, 6]. So it is absolutely essential to investigate the properties of mould fluxes simultaneously containing  $B_2O_3$  and/or  $TiO_2$  to develop the optimal fluorine free mould fluxes.

The performance of mold flux, such as heat transfer and lubricity, serves an important function to ensure the process stability of the continuous casting process and surface quality of products. And benign physio-chemical properties, which contribute the excellent performance of mold fluxes [1–9], are closely related to structure characteristic of slag. Knowledge of structure of molten slags is essential to understand the properties of slags. Consequently, it is practical importance of investigating the structure of mold slag to explore the appropriate physio-chemical properties of mold flux so as to guarantee the good performance, and thus achieve the purpose of controlling metallurgical processes.

For a better understanding of the structure characteristic of molten slag, a lot of analytical techniques have been developed and widely used, such as IR spectrum analysis, nuclear magnetic resonance (NMR), electronic probe rays microscopic analysis (EPMA), high temperature X-ray diffraction analysis, Raman spectroscopy, and so on. In comparison to other methods, Raman spectroscopy is with a lot of advantages in terms of micro-analysis, high analysis speed, high precision and accuracy, application to high-temperature condition and non-destruction [10–14]. Therefore, Raman spectroscopy has been successfully applied to detect the vibration mode of molecular or micro-structure units and has become a very popular technique to acquire the information of constituents and structure of materials [10–12].

It is effective to study the structure of high temperature melts through analyzing the Raman spectra of the corresponding glasses at room temperature in the fact that the spectra of glass and melts are similar based on the comparison of the infrared and Raman spectra of various silicate glasses and that of the corresponding melts by many researchers [13, 14]. Thus, the structure characteristic of  $B_2O_3$  and  $TiO_2$ -bearing fluoride-free mold flux has been investigated by analyzing the room-temperature Raman spectra of the glass systems in this work. Structural information of glass systems with variable  $TiO_2$  and  $B_2O_3$  content and different basicities ( $R = w(CaO)/w(SiO_2)$ ) were obtained by Raman spectra to examine the influences of  $TiO_2$ ,  $B_2O_3$  content and basicities on the structure of  $B_2O_3$  and  $TiO_2$ -bearing fluoride-free mold flux.

## 2 Experimental

### 2.1 Sample preparation

Analytical grade  $CaO$ ,  $SiO_2$ ,  $Al_2O_3$ ,  $MgO$ ,  $TiO_2$ ,  $Na_2CO_3$  and  $H_3BO_3$  were taken as raw materials, with  $Na_2CO_3$  and  $H_3BO_3$  being substitutes for  $Na_2O$  and  $B_2O_3$ , respectively. Table 1 presents the compositions (wt.%) of the glass samples investigated.

Glass samples with different  $TiO_2$ ,  $B_2O_3$  content and different basicities were prepared by the conventional melting and quenching method. Raw materials were mixed, taken into a platinum crucible and then melted in high temperature furnace at approximately 1573 K in air atmosphere. The samples were held at 1573 K for nearly 3 h to make sure complete melting and homogenization. After melting, the melts were quenched by water and then bulk glass samples are formed. These glass samples are proved to be amorphous by XRD (e.g. Figure 1).

Sample Number	basicity	CaO	SiO <sub>2</sub>	Al <sub>2</sub> O <sub>3</sub>	MgO	Na <sub>2</sub> O	TiO <sub>2</sub>	B <sub>2</sub> O <sub>3</sub>
1	R = 1	38	38	7	2	10	0	5
2		36.5	36.5	7	2	10	3	5
3		35.5	35.5	7	2	10	5	5
4		34.5	34.5	7	2	10	7	5
5		33	33	7	2	10	10	5
6		38	38	7	2	10	5	0
7		36.5	36.5	7	2	10	5	3
8		34.5	34.5	7	2	10	5	7
9		33	33	7	2	10	5	10
10	R = 1.2	38.7	32.3	7	2	10	5	5
11	R = 0.8	31.6	39.4	7	2	10	5	5

Table 1: Chemical compositions of experimental samples (wt.%)

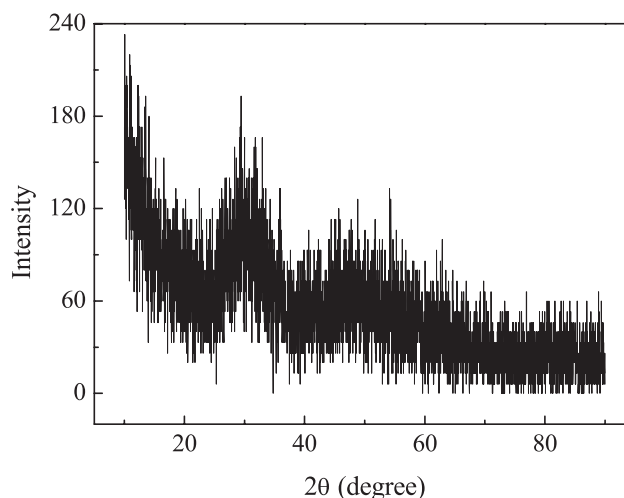


Fig. 1: A typical XRD pattern of the quenched sample

### 2.2 Raman spectroscopy measurement

Bulk glass samples were subjected to the Raman spectroscopy analysis. Raman spectra were acquired using a laser confocal micro-Raman spectrometer, JY-HR800, manufactured by Jobin Yvon of France. The experiments were carried out at room temperature using excitation wavelength of 532 nm and the light source was a semiconductor laser with power of 1 mw. The frequency band measured in this work ranged from 100 to 2000  $cm^{-1}$ .

### 3 Results and discussion

Figure 2, 3 and 4 present the room-temperature Raman spectra for glass samples with different contents of  $\text{TiO}_2$ ,  $\text{B}_2\text{O}_3$  and different basicities, respectively. All the backgrounds of the measured Raman signals have been

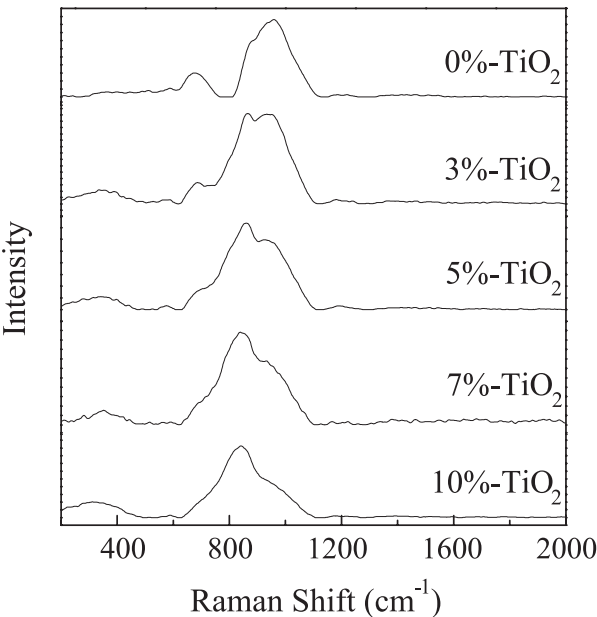


**Fig. 2:** Raman spectra for samples with different contents of  $\text{TiO}_2$  (No. 1, 2, 3, 4 and 5) at room temperature, after background subtraction

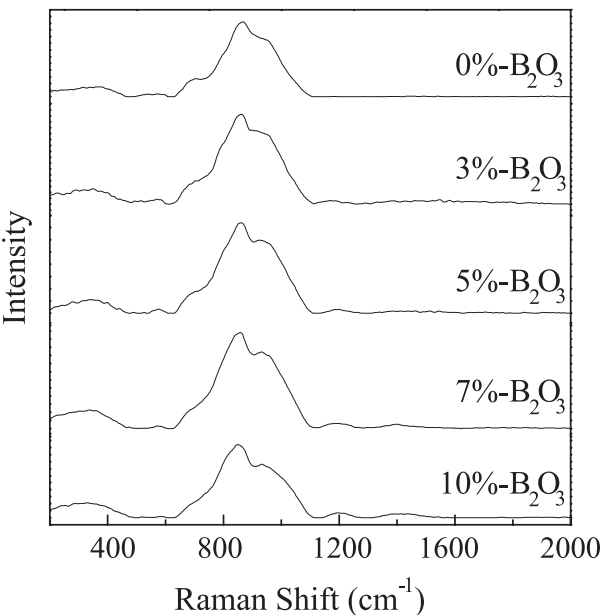


**Fig. 3:** Raman spectra for samples with different contents of  $\text{B}_2\text{O}_3$  (No. 3, 6, 7, 8 and 9) at room temperature, after background subtraction

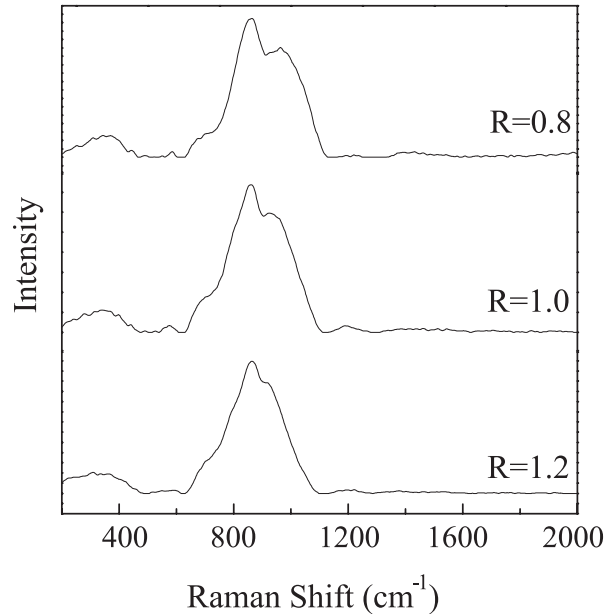


**Fig. 4:** Raman spectra for samples with different basicities (No. 3, 10 and 11) at room temperature, after background subtraction

Raman shift ( $\text{cm}^{-1}$ )	Raman assignments
677~680	O-Si-O deformation motion
690~700	Ti-O stretch vibrations of Ti in six-fold coordination ( $[\text{TiO}_6]$ )
~720	O-Ti-O deformation
~870	$\text{SiO}_4^{4-}$ stretching in monomer structure unit ( $\text{Q}^0$ ), or $\text{Q}^4(4\text{Al})$ structure unit
~950	$\text{SiO}_3^{2-}$ stretching with two bridging oxygen in chain structure unit ( $\text{Q}^2$ )
997~1037	Si-O-Si or (Si,Ti) coupling of stretch vibrations in sheet structure unit, or Si-O $^\circ$ antisymmetric stretching in any structural units that contain bridging oxygen
1192~1204	pyroborate group
1369~1379, 1435~1470	$\text{BO}_2\text{O}^-$ triangles units attached to the large borate group

**Table 2:** Assignments of Raman bands in spectra for the mold flux glass system

subtracted. All of the measured Raman spectra of glass samples are deconvolved by Gaussian-Deconvolution method similar to method by Mysen et al. [15] with the minimum correlation coefficient  $r^2 \geq 0.998$ . The deconvoluted results have been shown in Figure 5, 7 and 9. The focus of attention in this work is the middle and high frequency of the Raman spectra. Assignments of Raman peaks that are to the interest of present work have been listed in Table 2.

Figure 5 shows the deconvoluted results of Raman spectra for glass systems with different  $\text{TiO}_2$  content. It can be seen that in the  $\text{TiO}_2$ -free glass system (Figure 5 (a)),

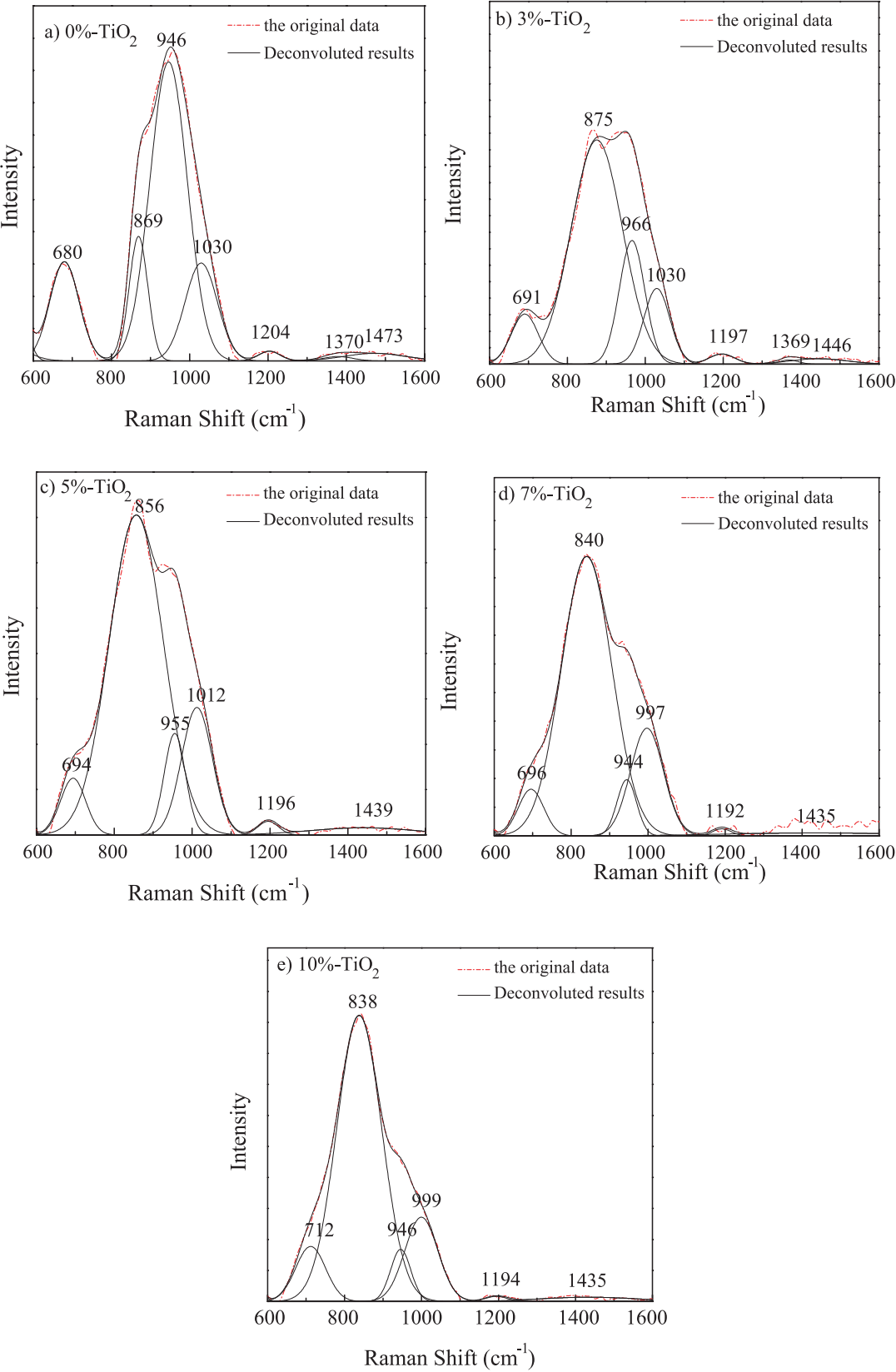


Fig. 5: Deconvoluted results of Raman spectra for samples with different  $\text{TiO}_2$  contents

there is a dominant Raman peak at approximately  $950\text{ cm}^{-1}$  which is due to  $\text{SiO}_3^{2-}$  stretching with  $\text{NBO}/\text{Si}=2$  (non-bridging oxygen per tetrahedrally coordinated cation) and referred to as  $\text{Q}^2$  (superscript refers to the number of bridging oxygen) species in a chain structure [16–21]. There are also three primary bands for sample without  $\text{TiO}_2$ , 679,  $\sim 870$  and  $1030\text{ cm}^{-1}$ . According to some previous researches [16–26], the band  $679\text{ cm}^{-1}$  could be assigned to O-Si-O deformation motion, the  $870\text{ cm}^{-1}$  band is assigned to  $\text{SiO}_4^{4-}$  stretching with  $\text{NBO}/\text{Si}=4$  and referred to as  $\text{Q}^0$  species in monomer structure, or it is due to  $\text{Q}^4(4\text{Al})$  structure unit, and the band at about  $1030\text{ cm}^{-1}$  is due to  $\text{Si-O}^\circ$  ( $\text{O}^\circ$ -bridging O atoms) antisymmetric stretching in any structural units that contain bridging oxygen but does not need be fully polymerized. It can be seen from Figure 5 that, as the addition of  $\text{TiO}_2$  increases, the band at about  $870\text{ cm}^{-1}$  becomes the dominant peak and simultaneously shifts toward low frequencies gradually, as  $856$ ,  $840$  and  $838\text{ cm}^{-1}$ , the  $1030\text{ cm}^{-1}$  band has shift toward low frequency, about  $1012$  and  $997\text{ cm}^{-1}$  respectively, and the  $\sim 950\text{ cm}^{-1}$  peak shows a decrease in intensity. Based on the reports of Mysen et al [22, 27], for Ti-bearing silicate melts, the bands at about  $830$  and  $810\text{ cm}^{-1}$  could correspond to the vibration of  $\text{Si-O}^{2-}$  structural unit and  $\text{Ti-O}^{2-}$  vibrations in the form of  $[\text{TiO}_4]$ , respectively, so it can be presumed that the emerging bands with increase of  $\text{TiO}_2$  content,  $856$ ,  $840$  and  $838\text{ cm}^{-1}$  may indicate mixing of the  $\text{Q}^0$  structure unit and  $[\text{TiO}_4]$  structural groups; the band in the range of  $997\sim 1030\text{ cm}^{-1}$  probably corresponds to the mixing of (Si,Ti) coupling of stretch vibrations in a sheet structure with randomly distribution of  $\text{Ti}^{4+}$  and  $\text{Si}^{4+}$  [22] and  $\text{Si-O}^\circ$  antisymmetric stretching in any structural units that contain bridging oxygen. Area ratios of the bands could reflect the abundance changes of different structure units, so the area fractions of bands in  $600\sim 1600\text{ cm}^{-1}$  are taken into consideration to describe the changes of structure groups in this work. Figure 6 presents the area fractions of bands in  $600\sim 1600\text{ cm}^{-1}$  as functions of  $\text{TiO}_2$  contents. It can be seen that with addition of  $\text{TiO}_2$ , the ratio of  $838\sim 875\text{ cm}^{-1}$  bands increases, the ratio of  $944\sim 966\text{ cm}^{-1}$  bands decreases and the ratio of  $997\sim 1030\text{ cm}^{-1}$  bands shows minor increase. That is to say,  $\text{TiO}_2$  exists in the system mainly in the form of  $[\text{TiO}_4]$  and the increase of  $\text{TiO}_2$  leads to the increase of ratio of  $\text{Q}^0$  structure unit and  $[\text{TiO}_4]$  structural groups, reduction of  $\text{Q}^2$  structure group, disappearance of the O-Si-O deformation. And simultaneously, some  $\text{TiO}_2$  enters into Si-O-Si network to form (Si,Ti) coupling of stretch vibrations in a sheet structure.

Besides, with increase of  $\text{TiO}_2$ , there appear a new band,  $690\sim 695\text{ cm}^{-1}$ , which shifts to  $712\text{ cm}^{-1}$  as the content

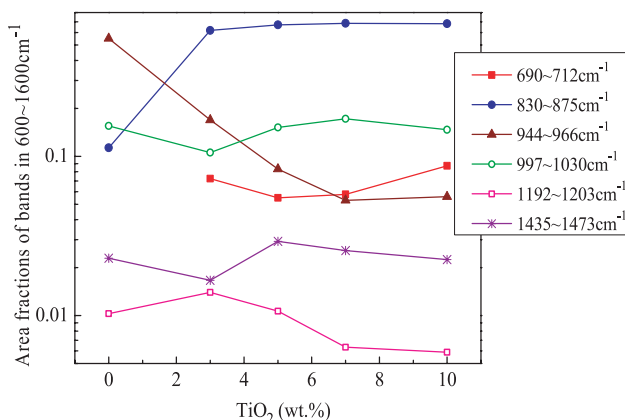


Fig. 6: Area fractions of bands in  $600\sim 1600\text{ cm}^{-1}$  as functions of  $\text{TiO}_2$  contents

of  $\text{TiO}_2$  increases to 10% in mass. According to Mysen et al [22], the band at approximately  $690\sim 695\text{ cm}^{-1}$  could be attributed to Ti-O stretch vibrations of Ti in six-fold coordination,  $[\text{TiO}_6]$ , and the band at  $720\text{ cm}^{-1}$  reflects the O-Ti-O deformation, so the band at  $712\text{ cm}^{-1}$  could be proposed to the mixing of the  $[\text{TiO}_6]$  structure unit and O-Ti-O deformation. There are also some changes for bands in high frequency with the increase of  $\text{TiO}_2$ . It can be seen from Figure 6 that, the ratio of Raman bands for small borate structure group, pyroborate ( $1192\sim 1204\text{ cm}^{-1}$ ), has somewhat decrease and the ratio of Raman bands for large borate structure group ( $1369\sim 1379$ ,  $1435\sim 1470\text{ cm}^{-1}$ ) decreases to a certain extent.

In general, it can be concluded that increasing the content of  $\text{TiO}_2$  leads to the appearance of  $[\text{TiO}_4]$  and  $[\text{TiO}_6]$  structure groups and  $[\text{TiO}_4]$  becomes the main structure unit in the system;  $\text{TiO}_2$  produces a certain destructive effect on Si-O-Si network structure as well as large borate group and conducive to the formation of some other complex structure groups, such as (Si,Ti) coupling in sheet unit.

The deconvoluted results of Raman spectra for glass samples with different  $\text{B}_2\text{O}_3$  content are presented in Figure 7. In the glass system without  $\text{B}_2\text{O}_3$  (Figure 7 (a)), the main structure units are mixing of the  $\text{Q}^0$  structure unit and  $[\text{TiO}_4]$  structural groups,  $\text{Q}^2$  in chain structure unit,  $[\text{TiO}_6]$  unit as well as mixing of (Si,Ti) coupling of stretch vibrations in a sheet structure and  $\text{Si-O}^\circ$  antisymmetric stretching in any structural units that contain bridging oxygen and. Figure 8 shows the area fractions of bands in  $600\sim 1600\text{ cm}^{-1}$  as functions of  $\text{B}_2\text{O}_3$  contents. It can be observed that, as the content of  $\text{B}_2\text{O}_3$  increases, the ratio of the dominant peak (in the vicinity of  $866\text{ cm}^{-1}$ ) decreases and the ratio of bands for sheet structure units ( $1010\sim 1014\text{ cm}^{-1}$ ) shows an increased tendency. It can be

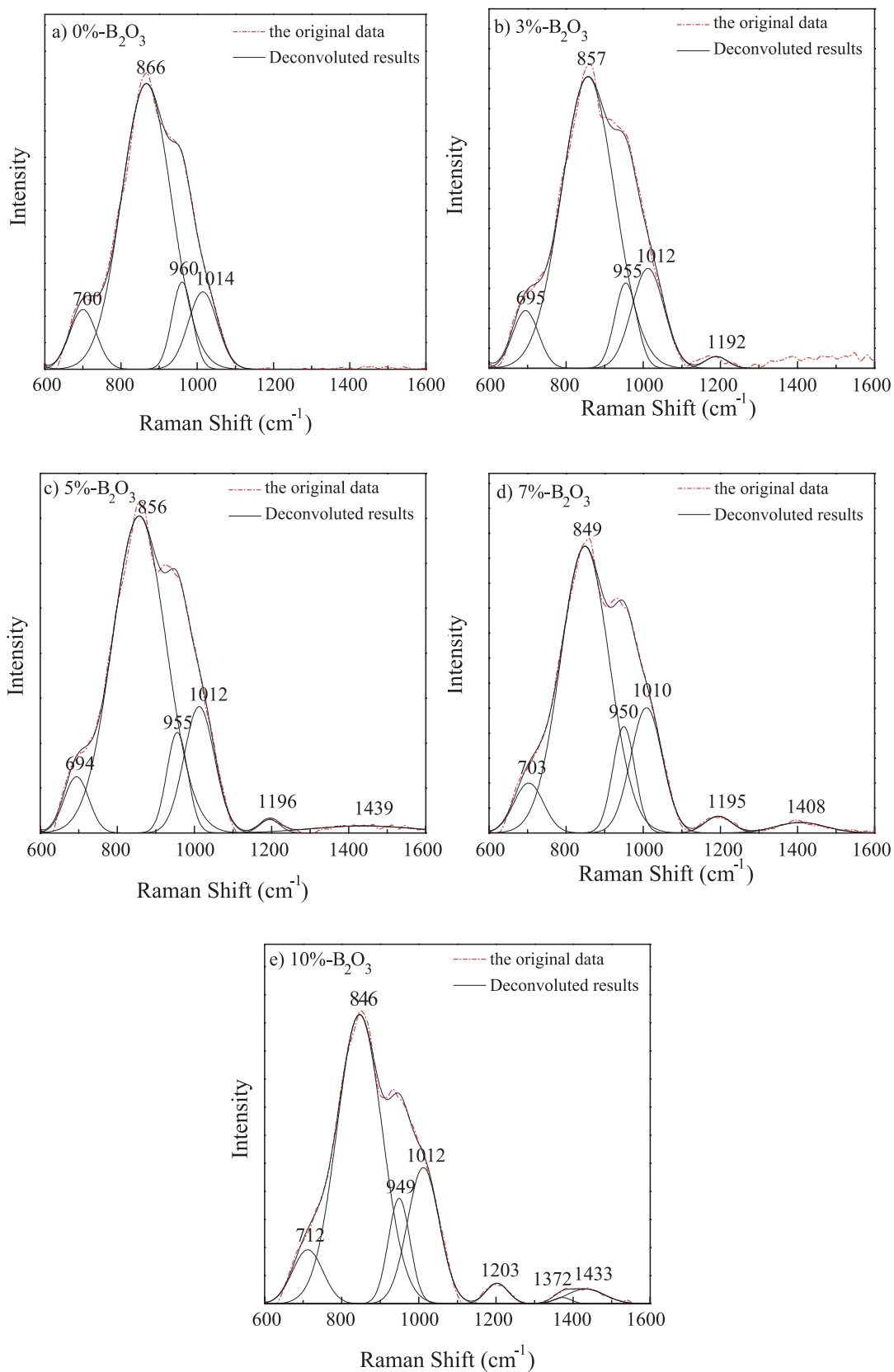


Fig. 7: Deconvoluted results of Raman spectra for glass samples with different  $B_2O_3$  content



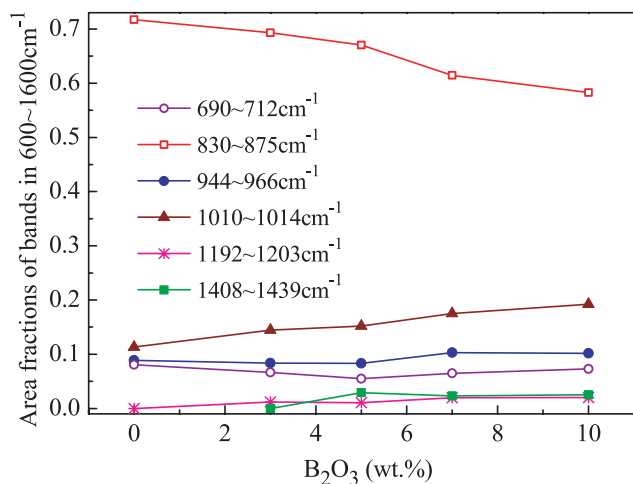


Fig. 8: Area fractions of bands in 600~1600 cm<sup>-1</sup> as functions of B<sub>2</sub>O<sub>3</sub> contents

seen from Figure 7 and Figure 8 that as minor B<sub>2</sub>O<sub>3</sub> is added into the system, such as 3% in mass, there firstly forms pyroborate structure unit, then, with the increase of B<sub>2</sub>O<sub>3</sub> content, BO<sub>2</sub>O<sup>-</sup> triangles units attached to the large borate group appear, and simultaneously the ratio of these borate structure groups increases to a certain extent. As the content of B<sub>2</sub>O<sub>3</sub> reaches 10% in mass, the band at about 695 cm<sup>-1</sup> move to the vicinity of 712 cm<sup>-1</sup>, that is, there forms some amount of O-Ti-O deformation due to the increase of B<sub>2</sub>O<sub>3</sub>. By and large, existence of B<sub>2</sub>O<sub>3</sub> leads to enhancement of polymerization degree of the slag system.

Figure 9 exhibits the deconvoluted results of Raman spectra for glass systems with different basicities. It can be seen that, when the basicity is 0.8, the structure groups exist in the system mainly in the form of mixing of the Q<sup>0</sup> structure unit and [TiO<sub>4</sub>] structural groups (856~864 cm<sup>-1</sup>),

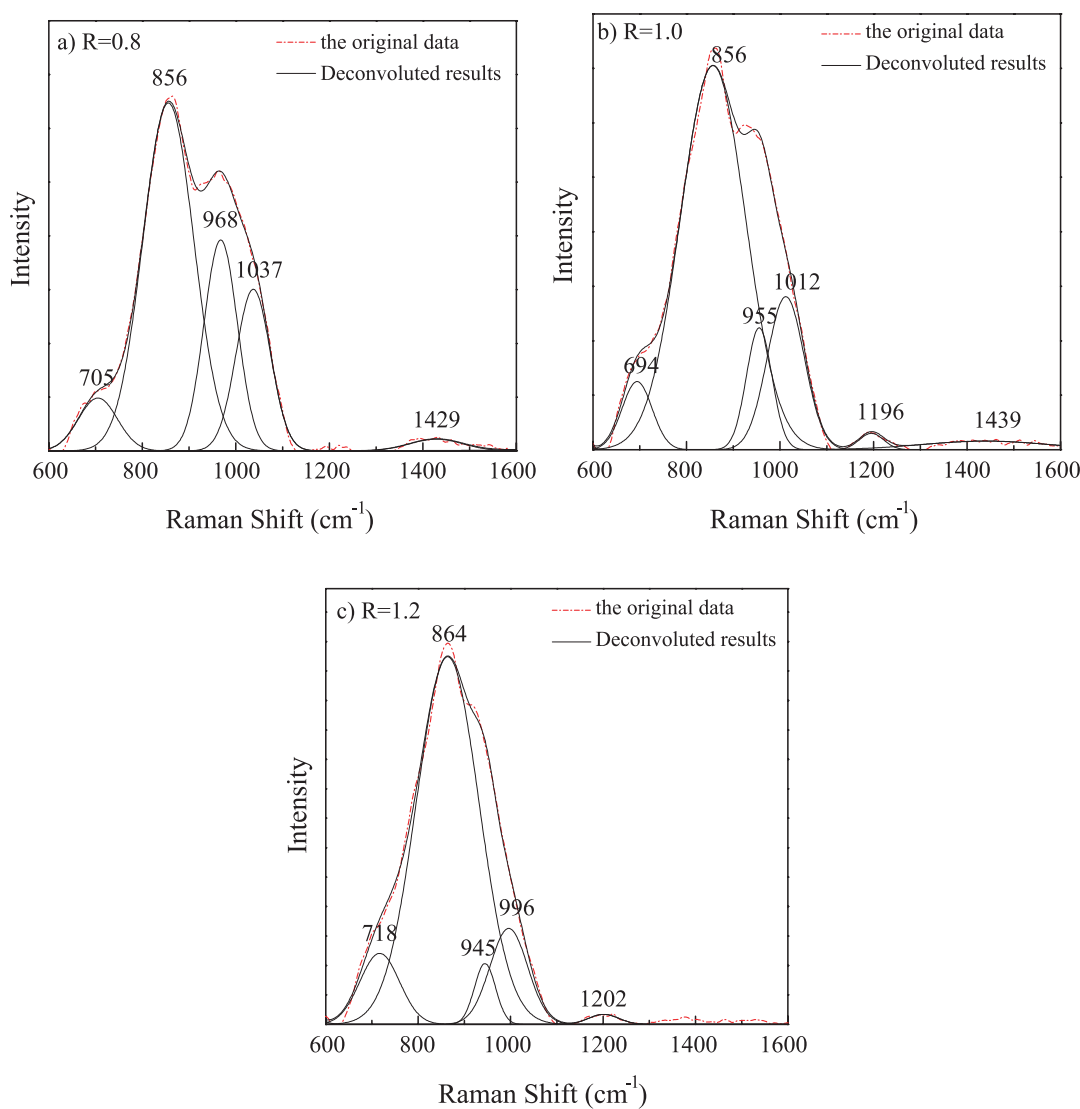


Fig. 9: Deconvoluted results of Raman spectra for glass samples with different basicities

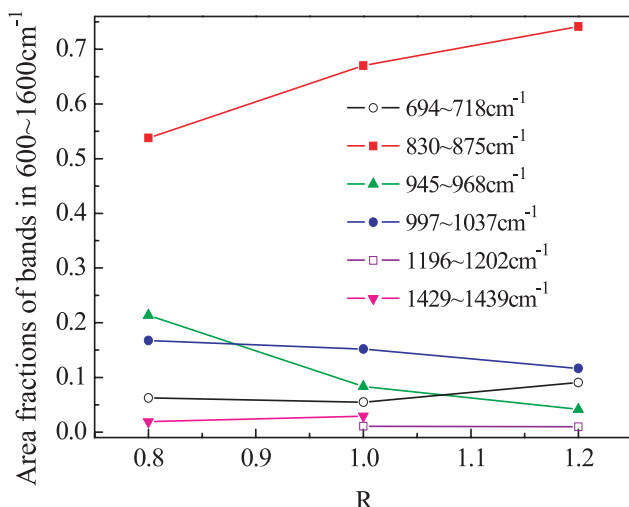


Fig. 10: Area fractions of bands in 600–1600 cm<sup>-1</sup> as functions of basicities

Q<sup>2</sup> in chain structure unit (945–968 cm<sup>-1</sup>), mixing of (Si,Ti) coupling of stretch vibrations in a sheet structure and Si-O<sup>-</sup> antisymmetric stretching in any structural units that contain bridging oxygen (996–1037 cm<sup>-1</sup>), and B<sub>2</sub>O<sub>3</sub> exists in the system primarily in the form of BO<sub>2</sub>O<sup>-</sup> triangles units attached to the large borate group. Figure 10 presents the area fractions of bands in 600–1600 cm<sup>-1</sup> as functions of basicities. It can be seen that, as the basicity increases, both the ratio of Q<sup>2</sup> in chain structure unit (945–968 cm<sup>-1</sup>) and sheet structure unit (996–1037 cm<sup>-1</sup>) decrease, while the ratio of mixing of the Q<sup>0</sup> structure unit and [TiO<sub>4</sub>] structural groups (856–864 cm<sup>-1</sup>) increases. It can be concluded that increasing the basicity produces a certain destructive effect on Si-O-Si network. Also, with the increase of basicity, and the band for BO<sub>2</sub>O<sup>-</sup> triangles units attached to the large borate group becomes too weak to be detected and along with the appearance of small borate group, pyroborate unit. That is, the increase of basicity causes simplification of borate network structure. Namely, the increase of basicity causes to negative effects on the borate network and Si-O-Si structure containing bridging oxygen.

## 4 Conclusions

The Raman spectroscopy technique has provided a deep insight into the structure of the B<sub>2</sub>O<sub>3</sub> and TiO<sub>2</sub>-bearing fluoride-free mold flux glass system. The increase of TiO<sub>2</sub> leads to the appearance of [TiO<sub>4</sub>], [TiO<sub>6</sub>] and O-Ti-O deformation structure groups. And TiO<sub>2</sub> exists in the slag mainly in the form of [TiO<sub>4</sub>]. TiO<sub>2</sub> weakens the Raman signals of Q<sup>2</sup>, O-Si-O deformation and BO<sub>2</sub>O<sup>-</sup> triangles units linked to

the large borate group, increases the ratio of mixing of the Q<sup>0</sup> structure unit and [TiO<sub>4</sub>] structural groups. That is to say, TiO<sub>2</sub> produces a certain destructive effect on Si-O-Si network structure as well as large borate group and conducive to the formation of some other complex structure groups, such as (Si,Ti) coupling in sheet structure unit.

With the increase of B<sub>2</sub>O<sub>3</sub>, the ratio of mixing of the Q<sup>0</sup> structure unit and [TiO<sub>4</sub>] structural group decreases and the ratio of sheet structure unit increase, and the peak for BO<sub>2</sub>O<sup>-</sup> unit attached to the large borate group shows an increase in intensity. Generally, existence of B<sub>2</sub>O<sub>3</sub> leads to the enhancement of polymerization degree of the slag system.

With the increase of basicity, the ratio of Q<sup>2</sup> and sheet structure unit decrease, and the ratio of mixing of the Q<sup>0</sup> structure unit and [TiO<sub>4</sub>] structural group increase. And BO<sub>2</sub>O<sup>-</sup> triangles units linked to the large borate group weaken, along with the appearance of pyroborate group. It suggests that the increase of basicity produces negative effects on the borate network and Si-O-Si structure containing bridging oxygen, and reduces the degree of polymerization of the system.

## Acknowledgements

The financial supports from NSFC (No. 50704002 and 51174018) and research funding for metallurgy of university of science and technology Beijing (YJ2011-003) are gratefully acknowledged.

Received: August 20, 2012. Accepted: October 13, 2012.

## References

- [1] M. Hayashi, N. Nabeshima, H. Fukuyama and K. Nagata, *ISIJ Int.*, **42** (2002), 352–358.
- [2] Guanghua WEN, Seetharaman SRIDHAR, Ping TANG, Xin QI and Yongqing LIU, *ISIJ Int.*, **47** (2007), 1117–1125.
- [3] Li Gui-rong, Wang Hong-ming, Dai Qi-xun, Zhao Yu-tao and Li Jing-sheng, *J. Iron Steel Res. Int.*, **14** (2007), 25–28.
- [4] Xin Qi, Guang-Hua Wen and Ping Tang, *J. Non-Cryst. Solids*, **354** (2008), 5444–5452.
- [5] S. Choi, D. Lee, D. Shin, S. Choi, J. Cho and J. Park., *J. Non-Cryst. Solids*, **345–346** (2004), 157–160.
- [6] A. B. Fox, K. C. Mills, D. Lever, C. Bezerra, C. Valadares, I. Unamuno, J. J. Laraudogoitia and J. Gisby, *ISIJ Int.*, **45** (2005), 1051–1058.
- [7] H. Nakada and K. Nagata, *ISIJ Int.*, **46** (2006), 441–449.
- [8] X. Qi, G. H. Wen and P. Tang, *J. Iron Steel Res., Int.*, **17** (2010), 06–10.
- [9] K. C. Mills and A. B. Fox, *ISIJ Int.*, **43** (2003), 1479–1486.



- [10] A. Grandjean, M. Malki, C. Simonnet, D. Manara and B. Penelon, *Phys. Rev. B*, **75** (2007), 054112-1–054112-7.
- [11] C. Gheorghies, I. Crudu, C. Teletin and C. Spanu, *J. Iron Steel Res. Int.*, **16** (2009), 12–16.
- [12] Andrzej Kudelski, *Talanta*, **76** (2008), 1–8.
- [13] S. Kashio, Y. Iguchi and T. Goto, *Trans. ISIJ.*, **20** (1980), 251–253.
- [14] F. A. Seifert, B. O. Mysen and D. Virgo, *Geochim. Cosmochim. Acta*, **45** (1981), 1879–1884.
- [15] B. O. Mysen, L. W. Finger, D. Virgo and F. A. Seifert, *Am. Mineral.*, **67** (1982), 686–695.
- [16] B. O. Mysen, D. Virgo and C. Scarfe, *Am. Mineral.*, **65** (1980), 690–710.
- [17] P. McMillan, *Am. Mineral.*, **69** (1984), 645–659.
- [18] P. McMillan, *Am. Mineral.*, **69** (1984), 622–644.
- [19] J. D. Frantz and B. O. Mysen, *Chem. Geol.*, **121** (1995), 155–176.
- [20] B. O. Mysen and J. D. Frantz, *Am. Mineral.*, **78** (1993), 699–709.
- [21] B. O. Mysen and J. D. Frantz, *Contrib. Mineral. Petrol.*, **117** (1994), 1–14.
- [22] B. O. Mysen, F. J. Ryerson and D. Virgo, *Am. Mineral.*, **65** (1980), 1150–1165.
- [23] Z. N. Utegulov, J. P. Wicksted and G. Q. Shen, *Phys. Chem. Glasses*, **45** (2004), 166–172.
- [24] B. O. Mysen, D. Virgo and F. A. Seifert, *Rev. Geophys.*, **20** (1982), 353–383.
- [25] Kohei Fukumia, Junji Hayakawaa and Toru Komiyama, *J. Non-Cryst. Solids*, **119** (1990), 297–302.
- [26] P. F. McMillan, G. H. Wolf and B. T. Poe, *Chem. Geol.*, **96** (1992), 351–366.
- [27] B. O. Mysen and Daniel Neuville, *Geochim. Cosmochim. Acta*, **59** (1995), 325–342.
- [28] B. N. Meera and J. Ramakrishna, *J. Non-Cryst. Solids*, **159** (1993), 1–21.
- [29] W. L. Konijnendijk and J. M. Stevels, *J. Non-Cryst. Solids*, **18** (1975), 307–331.
- [30] E. I. Kamitsos, M. A. Karakassides and G. D. Chryssikos, *Phys. Chem. glasses*, **30** (1989), 229–234.
- [31] E. I. Kamitsos, M. A. Karakassides and G. D. Chryssikos, *J. Phys. Chem.*, **91** (1987), 1073–1079.
- [32] G. D. Chryssikos, E. I. Kamitsos and W. M. Risen Jr., *J. Non-Cryst. Solids*, **93** (1987), 155–168.
- [33] G. Padmaja and P. Kistaiah, *J. Phys. Chem. A*, **113** (2009), 2397–2404.

